Physiological and behavioral sexual maturity of the female red deep-sea crab, *Chaceon quinquedens* (Smith, 1879), in the Mid-Atlantic Bight

Stephanie Martínez Rivera[1], William Christopher Long[2], and Bradley G. Stevens[1]

[1]*Department of Natural Sciences, University of Maryland Eastern Shore, Princess Anne, MD 21853, USA;* and

[2]*NOAA, National Marine Fisheries Service, Alaska Fisheries Science Center, Resource Assessment and Conservation Engineering Division, Kodiak Laboratory, 301 Research Ct., Kodiak, AK 99615, USA*

Correspondence: S. Martínez Rivera; email: smartinezrivera@outlook.com

(Received xxxx; accepted xxxx)

ABSTRACT

Red deep-sea crabs, *Chaceon quinquedens* (Smith, 1879), inhabit the continental shelf and slope of the western Atlantic and range from Nova Scotia to the Gulf of Mexico in water depths of 200–1800 m and water temperatures of 5–8° C. The objectives of this study were to describe physiological and behavioral maturity using ovary and oocyte development and morphological

features, respectively, to estimate the size at 50% sexual maturity (SM_{50}) for females in the Mid-Atlantic Bight. Samples were collected by trawling aboard NOAA research vessels in 2011–2013 and by traps aboard a commercial fishing vessel in 2014–2016. Histological analysis was used to describe ovarian and oocyte development stages. Five stages of ovarian development were described: 1) immature, 2) early maturing, 3) late maturing, 4) mature, and 5) redeveloping. A logistic model was used to estimate the SM_{50} using maximum likelihood methods. Physiological SM_{50} varied among geographic locations and was estimated at 61.2 mm CL and 70.8 mm CL for females collected near Hudson Canyon and Baltimore and Norfolk Canyons, respectively. Behavioral SM_{50} decreased with latitude and was estimated at 53.8 mm CL, 62.5 mm CL and 65.5 mm CL for Hudson, Baltimore, and Norfolk Canyons, respectively. Results implied asynchrony between physiological and behavioral sexual maturity, suggesting that mating occurs prior to completion of ovarian development. This study provides the first evidence of a latitudinal trend in sexual maturity for *C. quinquedens*.

Key words: brachyuran, oocyte, ovarian development, oocyte development, reproductive biology

INTRODUCTION

Red deep-sea crabs, *Chaceon quinquedens* (Smith, 1879), are found along the continental shelf and slope of the western Atlantic, ranging from Nova Scotia to the Gulf of Mexico in water depths of 200–1800 m and water temperatures of 5–8° C (Haefner & Musick, 1974; Wigley *et al.*, 1975; Steimle *et al.*, 2001). Red deep-sea crabs (RDSC) have been economically important since the 1970s, sustaining a small fishery in New England and the Mid-Atlantic (Wigley *et al.*,

1975; Wahle *et al.*, 2008). The Atlantic Red Crab Company (TARCC) is the only company fishing for RDSC and their main processing plant is located in New Bedford, Massachusetts. The current fishing grounds include Baltimore and Norfolk Canyons and fishing occurs year-round. The RDSC is a data-poor stock and research needs include estimation of reproductive parameters (Chute *et al.*, 2008). Studies of sexual maturity are needed to provide essential information for fisheries management and reproductive parameters for stock assessment models.

In crustaceans, sexual maturity can generally be divided into four categories: morphometric, physiological, behavioral, and functional maturity (Conan *et al.*, 2001; Haig *et al.*, 2016; Biscoito *et al.*, 2015; Pardo *et al.*, 2017; Robinson, 2008; González-Pisani *et al.*, 2017). Morphometric maturity indicates the presence of external secondary sexual characteristics necessary for reproduction and in females is commonly determined by using allometric relationships (e.g. abdomen width vs. carapace size) (Conan *et al.*, 2001). Physiological maturity is reached when the gonads are completely developed and ready to produce offspring (Haig *et al.*, 2016). Behavioral maturity is indicated by morphological features indicating successful mating; this includes sperm plugs and open gonopores in females (Haig *et al.*, 2016). Lastly, functional maturity in females indicates the presence of eggs attached to the pleopods (González-Pisani *et al.*, 2017). This study focuses on the physiological and behavioral sexual maturity of RDSC females.

Physiological maturity in females is commonly determined by examination of the ovary and oocyte development. The macroscopic condition of the ovary is an important element to characterize the stages of ovarian development, but for an adequate comprehension of the female reproductive cycle, it is necessary to describe oogenesis (Sharifian *et al.*, 2015). Oogenesis provides information about development and growth of the oocytes in the ovary, including yolk

accumulation in the oocyte, and changes in nucleus and ooplasm structures (Ravi *et al.*, 2012; Liu *et al.*, 2014; Sharifian *et al.*, 2015). Ovarian development has been studied for other geryonid crabs, including *Chaceon notialis* (Delgado & Defeo, 2004), *Chaceon fenneri* (Manning & Holthuis, 1984); Erdman & Blake, 1988; Hinsch, 1988), and *Chaceon maritae* (Manning & Holthuis, 1981; Melville-Smith, 1987), however, oocyte development was not very detailed described. In brachyurans, asynchrony between physiological and behavioral maturity may occur; hence, females might reach the pubertal molt (i.e. the molt to maturity, Sainte-Marie (1993), prior to ovarian maturation (Melville-Smith, 1987; Fernández-Vergaz *et al.*, 2000). Therefore, it is important to investigate both, physiological and behavioral maturity separately, to understand the reproductive cycle and population dynamics, and provide reliable estimates of size at maturity for RDSC.

Different types of sexual maturity have been used to estimate size at maturity for other crabs in the family Geryonidae, such as *Chaceon notialis* (Manning & Holthuis, 1989; Delgado & Defeo, 2004; Sant'Ana & Pezzuto, 2009), *Chaceon ramosae* (Manning, Tavares & Albuquerque, 1989; Pezzuto & Sant'Ana, 2009), and *Chaceon affinis* (A. Milne-Edwards & Bouvier, 1894; Fernández-Vergaz *et al.*, 2000; Pinho *et al.*, 2001). Size at sexual maturity for female RDSC was previously estimated between 65–75 mm in carapace length (CL) using the size distribution in which relative growth of the abdomen changes is associated with maturation of the vulvae, copulation and insemination, gonad development, and egg extrusion in the Chesapeake Bight (Haefner, 1977). Another study estimated size at sexual maturity at 61.6 mm CL using logistic regression on categories defined by vulva condition (Stevens & Guida, 2016) in the Mid-Atlantic Bight. Efforts to determine size at maturity for female RDSC using

allometric growth of the abdomen (i.e. morphometric maturity) have thus far been unsuccessful (Stevens & Guida, 2016).

Adequate fisheries management strategies rely on biological parameters and information on population dynamics of a species, which are not existing for RDSC. Lack of biological information for RDSC causes major uncertainties about the status of the current stock. This study is vital to begin understanding the reproductive biology of the current population, including ovarian development, sexual maturity types, and size at maturity. This information is necessary to understand the reproduction as well as population dynamics, growth characteristics and biological differences within the RDSC population (Sharifian *et al.*, 2015). In recognition of this, we decided to use histological observations of the ovarian and oocyte development to estimate physiological size at 50% sexual maturity (SM_{50}) for females. We also decided to use gonopore condition to estimate behavioral SM_{50} for comparisons between physiological and behavioral maturity.

MATERIALS AND METHODS

Sampling

Red deep-sea crabs for this study were collected in the Mid-Atlantic Bight (Fig. 1) during January of 2011 and 2012, and in July of 2013 aboard National Oceanic and Atmospheric Administration (NOAA) research vessels along the Hudson and Baltimore Canyons at depths >250 m by trawling (Stevens & Guida, 2016). During July and September of 2014 and July of 2015, sampling was conducted off Newport News, VA, along the Norfolk Canyon at depths >600 m aboard commercial vessels using traps, via collaboration with TARCC. The standard trap used by TARCC is a conical pot (120 cm diameter × 60 cm height) with ~7.6 cm nylon mesh and a top round entry (25 cm) (Tallack *et al.*, 2007), and traps are baited and tied to a string

in groups from 70 to 100 traps. In August of 2016, sampling was conducted off New Bedford, MA, along the Baltimore Canyon at depths >600 m by traps. Females were dissected on board and measured for carapace length (CL, from the rostral teeth to the center of the edge of the carapace) and carapace width (CW, including lateral spines) with a digital or manual caliper to the nearest 0.01 mm. During 2016, samples were collected in February, April, May, July, September, November, and December at the fishing ports in Newport News and Hampton, VA, from vessels fishing near the Norfolk Canyon at depths >600 m using traps. Females were kept alive in a cooler until measured and dissected at the laboratory, Paul S. Sarbanes Coastal Ecology Center (Berlin, MD), by placing them with the ventral surface up and creating a layer of ice packs between each layer of crabs. The size and color of ovaries, the presence of external eggs, and gonopore condition were recorded. Ovary size was classified as small, medium, or large using the midgut as a reference. An ovary was considered small if the midgut was completely visible, medium if the ovary was covering 1/2 of the midgut and large if the ovary was covering more than 3/4 of the midgut.

Physiological maturity

Physiological maturity was determined by histological examination of the ovaries of female crabs (Peemoeller & Stevens, 2013). Ovary samples (~1 cm^3) for histological analysis were preserved in 10% formalin and after a week transferred to 70% EtOH until processed. Tissues were dehydrated in a tissue processor (Tissue-Tek VIP-E150, Sakura Fineteck USA, Inc., Torrence, CA) consisting of a sequence of 70% EtOH, 95% EtOH, various concentrations of 100% EtOH, a clearing agent and melted paraffin. Then, tissues were embedded in paraffin using Tissue-Tek DRS (Sakura Fineteck USA, Inc., Torrence, CA), sectioned at 5–10 μm (depending on oocyte dimensions), stained with hematoxylin and eosin, and mounted in Permount. Ovary

sections were examined for the presence of oocytes, and digitally photographed at a magnification of 4X using two different microscopes: Leica M125 (Leica Microsystems, Wetzlar, Germany) stereo-zoom microscope, and Olympus DP73 digital camera mounted on an Olympus SXZ16 (Olympus Corporation, Tokyo, Japan) stereomicroscope. Higher magnification (10X) photos of oocytes and other cells in the ovary were taken with Olympus DP73 digital camera mounted on an Olympus BX41 (Olympus Corporation, Tokyo, Japan) compound microscope.

The areas of 30 randomly selected oocytes per female were measured from images using the ROI (Region of Interest) Manager tool in ImageJ Software (Schneider *et al.*, 2012). The scale was calibrated using an image of a micrometer at the same magnification and oocyte area was measured by drawing a line around the oocyte periphery. Area measurements were taken from oocytes sectioned through the nucleus, but if those were scarce, oocytes with part of the nucleus noticeable were measured. Only oocytes in the center of the images were measured, to reduce bias from a peripheral view, and different images were used until 30 measurements were recorded. Lastly, mean oocyte area was calculated for each female and then converted to mean oocyte diameter (calculated as $2\sqrt{A/\pi}$, where A is mean area). We decided to measure oocyte area and then use the conversion to diameter to reduce possible bias due to the sphere shape of oocytes (Swiney & Shirley, 2001).

The oocyte development was based on oocyte diameter, nuclear and ooplasm appearance, and yolk accumulation. Oocytes were categorized as one of the following: previtellogenic, early vitellogenic, late vitellogenic, vitellogenic, and atretic oocytes. The stages of ovarian development were described based on ovary size and color, and oocyte development. The stages of ovarian development were described as: 1) immature, 2) early maturing, 3) late maturing, 4)

mature, and 5) redeveloping. Presence of external eggs was used to distinguish between immature and redeveloping stages. The percentage of oocyte types was calculated for each stage of ovarian development. One-way analysis of variance was used to compare the mean oocyte diameters in each stage of ovarian development. Females were classified as physiologically mature if the ovary was in stages 2 through 5 (see above).

Behavioral maturity

Behavioral maturity for female crabs was defined based on the condition of their gonopores. Females with clean, closed gonopores were defined as immature, and those with blackened areas around the gonopores, indicative of prior copulation, were defined as mature.

Size at sexual maturity

The SM_{50} of female RDSC was estimated using a logistic model to describe the proportion of mature females, shown in Equation 1:

$$P_M = \frac{1}{1+\left(\frac{CL}{CL_{50}}\right)^{s}} \quad , \qquad (1)$$

where P_M is the probability of an individual being mature, CL is the carapace length, CL_{50} is the carapace length at 50% maturity (the SM_{50} in terms of CL), and s is the slope parameter. Physiological and behavioral maturity were fit separately using maximum likelihood and assuming a binomial distribution of data in R statistical software (R Development Core Team, 2011). Data were fit to a series of models in which CL_{50} or s were allowed to vary linearly with geographic locations (treated as a discrete variable). The best-fit model for SM_{50} was determined using the AIC_c (Akaike's Information Criterion corrected for sample size). Initial fits suggested that Baltimore and Norfolk Canyons had similar SM50s, so post hoc models were fit which included grouped areas by geographic location (i.e. north canyons vs. south

canyons); models were included in the analysis of physiological and behavioral maturity for comparison. Baltimore and Norfolk Canyons are the current fishing grounds for RDSC, hence, combining the sites in the model may be helpful for the fisheries management. All statistical results in this study are presented as mean ± standard deviation (mean ± SD).

RESULTS

A total of 681 female crabs were collected for the study across all years, seasons and geographic locations, ranging from 34.6 to 123.4 mm CL (Table 1, Fig. 2A). We observed that samples collected from Hudson Canyon had smaller CL sizes (69.9 ± 11.6 mm CL, $N = 64$) than Baltimore (81.0 ± 10.5 mm CL, $N = 254$) and Norfolk (87.5 ± 10.7 mm CL, $N = 363$) Canyons. Most samples were collected in fishing grounds (i.e. Baltimore and Norfolk Canyons) using round traps (Fig. 2B). It is important to mention that all samples from Hudson Canyon were collected by trawl, whereas, Baltimore and Norfolk Canyons were a combination of trawl (38% and 7%, respectively) and fishing traps (68% and 93%, respectively) (Table 1).

Ovarian development

We described five stages of ovarian development for female RDSC. The ovarian wall was formed by a thin epithelium and a thick layer of connective tissue and the ovary was formed by lobular areas where oogenesis occurs. The center of the ovary lobes was the germinal zone with new oogonia and oocytes developing, and, upon maturation, moving from the center to the periphery of the ovary (Fig. 3). The percentage of the types of oocytes varied between the stages of ovarian development. One-way analysis of variance showed a significant difference in the mean oocyte diameter of females between ovarian stages ($F = 684.3$; $P < 0.001$, $df = 4$).

Stage 1 (Immature): An ovary at early development was generally very thin or small in relation to the cephalothorax. The ovary color was white or ivory and smooth in appearance. The

ovary was frequently difficult to distinguish from the hepatopancreas in very small females. At this stage, present in the ovary are oogonial cells, primary and secondary oocytes, and previtellogenic oocytes located in the germinal zone (Fig. 3A). The primary and secondary oocytes are small and elliptical with a basophilic ooplasm and a large nucleus relative to the ooplasm (Fig. 4A). The previtellogenic oocytes have a moderate basophilia of the ooplasm, smaller nucleus and large nucleolus compare to primary and secondary oocytes (Fig. 4A). In this phase, the previtellogenic oocytes increase in size and mark the transition from basophilia to eosinophilia. As the previtellogenic oocytes continue to develop, they shift from the germinal zone to the periphery with follicle cells nearby. The ovary wall is thick and consisted of three distinguishable layers of epithelium and an underlying layer of thick connective tissue. Agglomerations of follicle cells were present in the ovary in this stage. Previtellogenic oocytes (88.6%) predominated at this stage, but oogonia, primary, and secondary oocytes (9.9%), and early vitellogenic oocytes (1.5%) were also present (Fig. 5A). The mean oocyte diameters ranged from 76.7 to 196.6 μm (164.6 ± 22.7 μm, $N = 43$, Fig. 5B). Due to absence of oocytes, measurements were not taken from three females. Female sizes ranged from 34.6 to 80.9 mm CL (65.7 ± 9.2 mm CL, $N = 46$, Fig. 6A, B).

Stage 2 (Early maturing): In this intermediate development stage, the ovary was small to medium in size; the color ranged from beige to light yellow to orange. There was a noticeable increase in ovary size compared to the previous stage, and ovaries covered part of the hepatopancreas, and the midgut was still visible. Lobulation and granular texture of the ovary were first observed at this stage. The ovary was surrounded by thin connective tissue, the ovary wall was not as evident as the previous stage, and the central lumen in the lobes was distinguishable (Fig. 3A). Early vitellogenic oocytes exhibited marginally granular and gradually

eosinophilic ooplasm due to vacuolated globules and small yolk platelets, as well as smaller basophilic nuclei (Fig. 4B). In the germinal zone, oogonial cells, primary and secondary oocytes (2.2%), and previtellogenic oocytes (44.7%) were observed. However, this stage was dominated by early vitellogenic oocytes (52.3%), and a few late vitellogenic oocytes (0.8%) were present, both were located in the periphery of the ovary with follicle cells nearby (Fig. 5A). At this stage, mean oocyte diameters ranged from 178.2 to 282.4 µm (227.8 ± 24.9 µm, $N = 101$, Fig. 5B). Female sizes in this stage ranged from 53.7 to 101.9 mm CL (81.5 ± 10.8 mm CL, $N = 101$, Fig. 6A, B).

Stage 3 (Late maturing): The ovary covered a portion of the hepatopancreas and midgut and ranged in size from medium to large. The color ranged from bright orange to dark orange to brown. The appearance of the ovary was granular with convoluted lobes. The ovary wall was very thin, and the germinal zone and central lumen decreases in area as the oocytes develop into late vitellogenic oocytes (Fig. 3B). The ovary was composed of oogonial cells, primary and secondary oocytes (0.9%), previtellogenic oocytes (18.1%), and early vitellogenic oocytes (17.0%) (Fig. 5A). The predominant late vitellogenic oocytes (52.2%) had an eosinophilic and granular ooplasm, muted eosinophilia in the nucleus, yolk platelets, and lipid droplets (Fig. 4C). A few late vitellogenic oocytes transitioning to mature oocytes (11.8%) were present. Yolk platelets, lipid droplets, and vacuolated globules increased in number, resulting in oocyte enlargement. At this time, we observed the presence of a chorion and tubular follicle cells enclosing the oocytes. The mean oocyte diameter ranged from 259.3 to 503.5µm (374.8 ± 71.1 µm, $N = 129$, Fig. 5B). Female sizes ranged from 62.9 to 109.2mm CL (87.1 ± 8.1 mm CL, $N = 129$, Fig. 6A, B).

Stage 4 (Mature): The ovary was large, highly lobulated, with a granulated texture and distinguishable oocytes. The ovary overlaid the midgut, heart, and portion of the hepatopancreas. The ovary color in this stage ranged from dark brown to red brown to purple. The ovary wall, germinal zone, and central lumen were faintly visible at this stage (Fig. 3C). During this stage, vitellogenic oocytes were completing maturation and becoming ready to be extruded and fertilized. Vitellogenic oocytes were filled with yolk platelets and lipid droplets and surrounded by tubular follicle cells (Fig. 4D). The size of the nucleus relative to the ooplasm was lower than previous stages. The ooplasm of the vitellogenic oocyte was very granular and eosinophilic due to yolk accumulation. The ovary was entirely mature with vitellogenic oocytes (85.2%) and a few late vitellogenic oocytes (1.9%). Oogonial cells, primary and secondary oocytes (0.8%), previtellogenic oocytes (11.8%) and a few early vitellogenic oocytes (0.3%) were found in the ovary indicating the development of a new cohort (Fig. 5A). This suggests that the development of oocytes in the ovary is continuous. The mean oocyte diameter ranged from 504.3 to 671.4 μm (578.6 ± 44.2 mm CL, $N = 48$, Fig. 5B). Female sizes ranged from 77.6 to 110.9 mm CL (92.0 ± 8.2 mm CL, $N = 48$, Fig. 6A, B).

Stage 5 (Redeveloping): After egg extrusion, the ovary underwent severe reduction in size and became smooth-textured, and the color varied from ivory to beige. This stage is very similar to the immature stage except all the females were ovigerous. During this stage, oocytes that had not been extruded from the ovary were being resorbed. Atretic oocytes had a degenerating ooplasm with vacuoles, a thick surrounding membrane surrounded by follicle cells, and an amorphic shape (Fig. 4E). Atretic oocytes (2.5%) at different degrees of resorption were found in the ovary, although the ovary was dominated by previtellogenic oocytes (85.2%) with few oogonia, primary and secondary oocytes (6.5%), and early vitellogenic oocytes (5.8%) (Fig.

5A). The mean oocyte diameter ranged from 120.3 to 546.9 μm (191.1 ± 50.4 mm CL, $N = 37$, Fig. 5B). Ovigerous female sizes ranged from 59.7 to 110.7 mm CL (88.6 ± 7.9 mm CL, $N = 37$, Fig. 6A, B).

Physiological maturity

A total of 435 female RDSC sampled in 2011–2016 were individually analyzed to estimate size at physiological sexual maturity. The best-fit model showed geographical differences in the estimated value of physiological SM_{50} and slopes (Table 2) and there was no support for the null model of no difference among the sites. There were a total of four models that had $\Delta AIC_c < 2$ indicating that all had similar levels of support; since all show the same trend of latitudinal differences in the SM_{50} we present the best fit model which shows a difference among the north and south canyons and note that there is evidence that all three differ. In the best-fit model (i.e. model 1 in Table 2), physiological SM_{50} was estimated at 61.2 mm CL (CI ± 3.8) for Hudson Canyon (i.e. north site), and 70.8 mm CL (CI ± 1.9) for Baltimore and Norfolk Canyons (i.e. south sites) (Fig. 7A, B). Physiologically mature females (PMF, $N = 389$) ranged from 53.7 to 110.9 mm CL (86.7 ± 9.5 mm CL, Fig. 8). The mean size of PMF by geographic locations was 73.7, 85.4 and 89.8 mm CL for Hudson, Baltimore, and Norfolk Canyons, respectively. For physiologically immature females (PIMF, $N = 46$), the CL range was 34.6–80.9 mm (65.7 ± 9.2 mm CL, Fig. 8) and the mean size was 62.8, 65.7 and 68.0 mm CL for Hudson, Baltimore, and Norfolk Canyons, respectively.

Behavioral maturity

A total of 633 female RDSC sampled in 2012–2016 were individually analyzed to estimate size at behavioral maturity using condition of the gonopores. Similar to our physiological maturity analysis, the best-fit model (i.e. model 1 in Table 3) showed difference in the SM_{50} among all

297 sites with no support for the null model of no difference (Table 3); in addition, there were two
298 other models (i.e. model 2 and 3 in Table 3) that had ΔAICc < 2 with good support for a slightly
299 simpler model showing a general difference between north and south canyons. Female
300 behavioral SM_{50} was estimated at 53.9 mm CL (CI ± 7.0) for Hudson Canyon, 62.5 mm CL (CI
301 ± 2.9) for Baltimore Canyon, and 65.5 mm CL (CI ± 3.0) for Norfolk Canyon (Fig. 5C–E).
302 Behavioral mature females (BMF, *N* = 596) ranged from 53.7 to 123.4 mm CL (86.0 ± 9.3 mm
303 CL, Fig. 8). The mean size of BMF by geographic locations was 68.1, 82.7, and 88.9 mm CL for
304 Hudson, Baltimore, and Norfolk Canyons, respectively. Behavioral immature females (BIMF, *N*
305 = 37) ranged from 34.6 to 74.4 mm CL (56.2 ± 9.9 mm CL, Fig. 8). The BIMF mean size was
306 43.1, 56.7, and 58.7 mm CL for Hudson, Baltimore, and Norfolk Canyons, respectively.

307 DISCUSSION

308 Five stages of ovarian development were described for RDSC: 1) immature, 2) early maturing, 3)
309 late maturing, 4) mature, and 5) redeveloping. Understanding ovarian development is crucial to
310 adequately understanding the population dynamics of a species (Sharifian *et al.*, 2015). The
311 stages of ovarian development in this study are similar to those described for other species of
312 geryonid crabs (Melville-Smith, 1987; Delgado & Defeo, 2004; Fernández-Vergaz *et al.*, 2000).
313 Five stages of ovarian development using oocyte diameter were previously defined for RDSC
314 (Haefner, 1977); however, measurements of oocyte diameter calculated from oocyte area used in
315 this study increase the level of precision (Crisp *et al.*, 2017). The ovarian development of RDSC
316 appeared to have a continuous development of oocytes in the ovary, due to the presence of
317 oogonia, primary and secondary oocytes, in all five ovarian stages (Fig. 5A). The overlap
318 between ovarian stages and crab size across the size range of females suggests that ovarian

development in RDSC is a slow and prolong process (Fig. 6B), which is consistent with a slow-growing brachyuran in the deep-sea environment (Hastie, 1995).

As oocyte development progressed, the ovary increased in size and changed in color; however, ovary color overlapped across ovarian stages. Biochemical composition and endocrinology studies of the ovary may clarify the pigmentation changes during development. By examining the oocyte development, we were able to identify the production of a new cohort in the ovary during stages 3 and 4, demonstrating that oogenesis continues before oviposition occurs; therefore, after oviposition the ovary is occupied almost completely by previtellogenic oocytes (i.e. stage 5). The oogonia cells and previtellogenic oocytes had a basophilic ooplasm, whereas the oocytes from early vitellogenesis to vitellogenesis became gradually eosinophilic, similar to *Callinectes sapidus* Rathbun, 1896 (Brown, 2009), *Portunus pelagicus* (Linnaeus, 1758; Ravi *et al.*, 2012) and four Mithracidae species (Mollemberg *et al.*, 2017). The reason for this difference in staining is mainly attributed to yolk accumulation in the oocytes (Smija & Sudha Devi, 2015).

Our SM_{50} estimates of RDSC are lower than previously reported by Haefner (1977) suggesting that females in the current population may be mating at smaller sizes. All the females <70 mm CL of RDSC from the Mid-Atlantic Bight had gonopores with intact margins (i.e. were BIMF) (Haefner, 1977); however, in this study only 53% of females <70 mm CL were BIMF, suggesting that size of BMF has possibly decreased. Considering that 95% of females ≥70 mm CL were BMF in this study, the current acceptable size to harvest males is 75 mm CL, from 94 mm CW in Chute *et al.* (2008), using the equation for RDSC by Stevens & Guida (2016), and males have to be 50% larger than females for mating (Wahle *et al.*, 2008); thus, it is possible that females may not find males of appropriate size for mating. Further investigation is needed to

342 explore the possibility that the differences in size at maturity between Haefner's (1977) study
343 and ours could be a consequence of removing large males from the population during 40 years of
344 fishing.

345 The latitudinal trend in both physiological and behavioral SM_{50} estimates for female
346 RDSC, increasing from north (Hudson Canyon) to south (Norfolk Canyon), suggests there are
347 differences in population dynamics by geographical site. The mean CL of female crab was
348 significantly greater at Norfolk Canyon than at any of the other sites (Stevens & Guida, 2016),
349 which is consistent with our SM_{50} estimates. The RDSC fishery is managed as a single stock but
350 this information suggests differences in the reproduction of RDSC due to geographic locations,
351 therefore, stock boundaries may have to be taken into consideration. Latitudinal clines in size at
352 maturity have been attributed to phenotypic plasticity due to environmental variations (Orensanz
353 *et al.*, 2007). The decline in size at maturity with increasing latitudes is the inverse of
354 Bergmann's rule, which establishes that higher latitudes and colder temperature have large-size
355 animals, and lower latitudes and warmer temperatures have small-size animals (Meiri, 2011).
356 This inverse of Bergmann's rule was described for female snow crabs (*Chionoecetes opilio* (O.
357 Fabricius, 1788) in the eastern Bering Sea (Orensanz *et al.*, 2007). Latitudinal clines in size at
358 maturity may denote changes in life history and population dynamics in a species (Hines, 1989).
359 The cause of geographic variations in size at sexual maturity in RDSC merits further
360 investigation since our study present limitations in size frequency and sample size among
361 geographic locations (Table 1, Fig. 2) that may be a result of size selectivity of the sampling
362 methods.

363 Size at sexual maturity for RDSC indicated asynchrony between physiological and
364 behavioral maturity, implying that mating may occur prior to completion of ovarian

365 development. Analysis of physiologically and behaviorally mature females showed that 58% of
366 females with a stage 1 ovary and 100% of females with a stage 2 ovary were BMF, suggesting
367 they are able to mate before completing the ovarian maturation, hence, they present asynchrony
368 between physiological and behavioral maturity. The red crab, *C. maritae*, from South West
369 Africa is asynchronous (Melville-Smith, 1987); in contrast, *C. notialis* from the southwestern
370 Atlantic Ocean (Delgado & Defeo, 2004) exhibited synchrony. The females of *C. affinis* from
371 the Canary Islands reach morphometric maturity before completing physiological maturation
372 (Fernández-Vergaz *et al.*, 2000), similar to our findings.

373 Fisheries management relies on biological information such as sexual maturity to
374 incorporate the population dynamics of a species into stock assessment. We recommend that
375 special attention be given to the geographical differences in SM_{50} within the RDSC population,
376 in order to understand stock structure and improve management. Updated estimates of SM_{50} for
377 the current population of RDSC suggest that size at maturity has declined over time, possibly as
378 a result of fishing and different stocks defined by geographic range. This study provides valuable
379 information for the development of appropriate management strategies for RDSC.

380 ACKNOWLEDGMENTS

381 We thank the Atlantic Red Crab Company for allowing us to sample during fishing trips and the
382 assistance provided aboard the vessel. We are thankful to Shadaesha Green, Indu Sharma, and
383 Justin Wilson for their participation during the sample collection. We wish to acknowledge the
384 help provided by Samantha Peart with the histological analysis. Special thanks to Andrés G.
385 Morales-Núñez for permitting us use of his laboratory equipment. We are grateful for the
386 contributions by the anonymous reviewers. Funding for this research was provided by NOAA
387 grants NA11SEC4810002 and NA16SEC4810007 to the Living Marine Resources Cooperative

Science Center at University of Maryland Eastern Shore. Reference to trade names or commercial firms does not imply endorsement by the National Marine Fisheries Service, NOAA. The scientific results and conclusions, as well as any views or opinions expressed herein, are those of the author(s) and do not necessarily reflect those of NOAA or the Department of Commerce.

REFERENCES

Biscoito, M., Freitas, M., Pajuelo, J.G., Triay-Portella, R., Santana, J.I., Costa, A.L., Delgado, J. & González, J.A. 2015. Sex structure, depth distribution, intermoult period and reproductive pattern of the deep-sea red crab *Chaceon affinis* (Brachyura, Geryonidae) in two populations in the north-eastern Atlantic. *Deep-Sea Research I*, **95**: 99–114.

Brown, C.E. 2009. *Ovarian morphology, oogenesis, and changes through the annual reproductive cycle of the female blue crab,* Callinectes sapidus *Rathbun, in Tampa Bay*. M.S. thesis, University of South Florida, Florida, United States.

Chute, A., Jacobson, L. & Rago, P. 2008. Deep sea red crab. Northeast Data Poor Stocks Working Group Meeting, NOAA Northeast Fisheries Science Center, Massachusetts, United States.

Conan, G.Y., Comeau, M. & Moriyasu, M. 2001. Are morphometrical approaches appropriate to establish size at maturity for male American lobster, *Homarus americanus*? *Journal of Crustacean Biology*, **21**: 937–947.

Crisp, J.A., D'Souza, F.M.L., Tweedley, J.R., Partridge, G.J. & Moheimani, N.R. 2017. Quantitative determination of ovarian development in penaeid prawns (Decapoda: Penaeidae). *Journal of Crustacean Biology*, **37**: 81–89.

410 Delgado, E. & Defeo, O. 2004. Sexual maturity in females of deep-sea red crab *Chaceon notialis*
411 (Brachyura, Geryonidae) in the southwestern Atlantic Ocean. *Invertebrate Reproduction*
412 *and Development*, **46**: 55–62.
413 Erdman, R.B. & Blake, N.J. 1988. Reproductive biology of female golden crabs *Geryon fenneri*
414 Manning and Holthuis, from southeastern Florida. *Journal of Crustacean Biology*, **8**:
415 392–400.
416 Fabricius, O. 1788. Beskrivelse over den store Gronlandske Krabbe. *Nye Samling af det*
417 *Kongelige Danske Videnskabers Selskabs Skrifter*, **3**: 181–190, 1 pl.
418 Fernández-Vergaz, V., López Abellán, L.J. & Balguerías, E. 2000. Morphometric, functional and
419 sexual maturity of the deep-sea red crab *Chaceon affinis* inhabiting Canary Island waters:
420 chronology of maturation. *Marine Ecology Progress Series*, **204**: 169–178.
421 González-Pisani, X., Barón, P.J. & López Greco, L.S. 2017. Integrated analysis of sexual
422 maturation through successive growth instars in the spider crab *Leurocyclus tuberculosus*
423 (Decapoda: Majoidea). *Canadian Journal of Zoology*, **95**: 473–483.
424 dx.doi.org/10.1139/cjz-2016-0034
425 Haefner, P.A., & Musick, J.A. 1974. Observations on distribution and abundance of red crabs in
426 Norfolk Canyon and adjacent continental slope. *Marine Fisheries Review*, **36**: 31–34.
427 Haefner, Jr., P. A. 1977. Reproductive biology of the female deep-sea red crab, *Geryon*
428 *quinquedens*, from the Chesapeake Bight. *Fishery Bulletin*, *U.S.* **75**: 91–102.
429 Haig, J.A., Bakke, S., Bell, M.C., Bloor, I.S.M., Cohen, M., Coleman, M., Dignan, S., Kaiser,
430 M.J., Pantin, J.R., Roach, M., Salomonsen, H. & Tully, O. 2016. Reproductive traits and
431 factors affecting the size at maturity of *Cancer pagurus* across Northern Europe. *ICES*
432 *Journal of Marine Science*, [doi:10.1093/icesjms/fsw081].

433 Hastie, L.C. 1995. Deep-water geryonid crabs: a continental slope resource. In: *Oceanography*
434 *and Marine Biology: an Annual Review* (A.D. Ansell, R.N. Gibson, & M. Barnes, eds.),
435 pp. 561–584. UCL Press, London, UK.
436 Hines, A. H. 1989. Geographic variation in size at maturity in brachyuran crabs. *Bulletin of*
437 *Marine Science*, **45**: 356–368.
438 Hinsch, G.W. 1988. Morphology of the reproductive tract and seasonality of reproduction in the
439 golden crab *Geryon fenneri* from the eastern Gulf of Mexico. *Journal of Crustacean*
440 *Biology*, **8**: 254–261.
441 Linnaeus, C. 1758. *Systema Naturae per regna tria naturae, secundum classes, ordines, genera,*
442 *species, cum characteribus, differentiis, synonymis, locis*. Editio decima, reformata.
443 Laurentius Salvius: Holmiae ii.
444 Liu, Z., Wu, X., Wang, W., Yan, B. & Cheng, Y. 2014. Size distribution and monthly variation
445 of ovarian development for the female blue swimmer crab, *Portunus pelagicus* in Beibu
446 Gulf, off south China. *Scientia Marina*, **78**(2): 257–268.
447 doi:http://dx.doi.org/10.3989/scimar.03919.24A
448 Manning, R.B. & Holthuis, L.B. 1981. West African brachyuran crabs (Crustacea: Decapoda).
449 *Smithsonian Contributions to Zoology*, **306**: 1–379.
450 Manning, R.B. & Holthuis, L.B. 1984. *Geryon fenneri*, a new deep-water crab from Florida
451 (Crustacea: Decapoda: Geryonidae). *Proceedings of the Biological Society of*
452 *Washington*, **97**: 666–673.
453 Manning, R.B. & Holthuis, L.B. 1989. Two new genera and nine new species of Geryonid crabs
454 (Crustacea, Decapoda, Geryonidae). *Proceedings of the Biological Society of*
455 *Washington*, **102**: 50–77.

456 Manning, R.B., Tavares, M.S. & Albuquerque, E.F. 1989. *Chaceon ramosae*, a new deep-water
457 crab from Brazil (Crustacea: Decapoda: Geryonidae). *Proceedings of the Biological*
458 *Society of Washington*, **102**: 646–650.
459 Meiri, S. 2011. Bergmann's rule-what's in a name? *Global Ecology and Biogeography*, **20**: 203–
460 207.
461 Melville-Smith, R. 1987. The reproductive biology of *Geryon maritae* (Decapoda, Brachyura)
462 off South West Africa/Namibia. *Crustaceana*, **53**: 259–275.
463 Milne-Edwards, A. & Bouvier, E.L. 1894. Brachyures et anomoures. Crustacés décapodes
464 provenant des campagnes du yacht l'Hirondelle (1886, 1887, 1888). *Résultats des*
465 *campagnes scientifiques accomplies sur son yacht par Albert Ier, Prince Souverain de*
466 *Monaco*, **7**: 1–112.
467 Mollemberg, M., Zara, F.J. & Santana, W. 2017. Morphology and ultrastructure of the adult
468 ovarian cycle in Mithracidae (Crustacea, Decapoda, Brachyura, Majoidea). *Helgoland*
469 *Marine Research*, **71**:14 [doi:10.1186/s10152-017-0494-y].
470 Orensanz, J.M. (Lobo), Ernst, B. & Armstrong, D.A. 2007. Variation of female size and stage at
471 maturity in snow crab (*Chionoecetes opilio*) (Brachyura: Majidae) from the eastern
472 Bering Sea. *Journal of Crustacean Biology*, **27**: 576–591.
473 Pardo, L.M., Ceroni, C., Riveros, M.P., Ernst, B. & Pino, J. Morphology of seminal receptacle of
474 the harvested golden crab *Chaceon chilensis* and its implication in the fertilization
475 process. *Invertebrate Biology*, **136**(2): 199–206.
476 Peemoeller, B-J. & Stevens, B.G. 2013. Age, size, and sexual maturity of channeled whelk
477 (*Busycotypus canaliculatus*) in Buzzards Bay, Massachusetts. *Fishery Bulletin*, **111**(3):
478 265–278.

479 Pezzuto, P.R. & Sant'Ana, R. 2009. Sexual maturity of the deep-sea royal crab *Chaceon*
480 *ramosae* Manning, Tavares & Albuquerque, 1989 (Brachyura: Geryonidae) in southern
481 Brazil. *Latin American Journal of Aquatic Research*, **37** [doi:10.3856/vol37-issue3-
482 fulltext-2].
483 Pinho, M.R., Gonçalves, J.M., Martins, H.R. & Menezes, G.M. 2001. Some aspects of the
484 biology of the deep-water crab, *Chaceon affinis* (Milne-Edwards and Bouvier, 1894) off
485 the Azores. *Fisheries Research*, **51**: 283–295.
486 Rathbun, M.J. 1896. The genus *Callinectes*. Proceedings of the United States National Museum.
487 **18**(1070): 349-375.
488 Ravi, R., Manisseri, M.K. & Sanil, N.K. 2012. Ovarian maturation and oogenesis in the blue
489 swimmer crab, *Portunus pelagicus* (Decapoda: Portunidae). *Acta Zoologica*, **00**: 1–9
490 [doi:10.1111/j.1463-6395.20].
491 Robinson, M. 2008. Minimum landing size for Northeast Atlantic stocks of deep-water red crab,
492 *Chaceon affinis* (Milne Edwards and Bouvier, 1894). *ICES Journal of Marine Science*,
493 **65**: 148–154.
494 Sainte-Marie, B. 1993. Reproductive cycle and fecundity of primiparous and multiparous female
495 snow crab, *Chionoecetes opilio*, in the Northwest Gulf of Saint Lawrence. *Canadian*
496 *Journal of Fisheries and Aquatic Sciences*, 50: 2147–2156.
497 Sant'Ana, R. & Pezzuto, P.R. 2009. Sexual maturity of the deep-sea red crab *Chaceon notialis*
498 Manning & Holthuis, 1989 (Brachyura: Geryonidae) in southern Brazil. *Latin American*
499 *Journal of Aquatic Research*, **37**: 429–442.
500 Schneider, C.A., Rasband, W.S. & Eliceiri, K.W. 2012. NIH Image to ImageJ: 25 years of Image
501 Analysis. *Nature methods*, **9**: 671–675.

502 Sharifian, S., Kamrani, E., Safaie, M. & Sharifian, S. 2015. Oogenesis and ovarian development
503 in the freshwater crab *Sodhiana iranica* from south of Iran. *Tissue & Cell*, **47**: 213–220.
504 Smija, M.K. & Sudha Devi, A.R. 2015. Oocyte development and female reproductive cycle in
505 the freshwater crab *Travancoriana schirnerae*. *Turkish Journal of Fisheries and Aquatic*
506 *Sciences*, **15**: 691–702.
507 Smith, S.I. 1879. The stalk-eyed crustaceans of the Atlantic coast of North America north of
508 Cape Cod. *Transactions of the Connecticut Academy of Arts and Sciences*, **5**: 27–136.
509 Steimle, F.W., Zetlin, C. A. & Chang, S. 2001. Essential Fish Habitat Source Document: red
510 deepsea crab, *Chaceon (Geryon) quinquedens*, life history and habitat characteristics.
511 NOAA Technical Memorandum NMFS-NEFSC-163, 27 p.
512 Stevens, B.G. & Guida, V. 2016. Demographics, morphometrics, depth, and temperature
513 distribution of red deepsea crabs *Chaceon quinquedens* at four sites in the Mid-Atlantic
514 Bight. *Fishery Bulletin*, U.S. **114**: 343–359.
515 Swiney, K.M. & Shirley, T.C. 2001. Gonad development of southeastern Alaskan Dungeness
516 crab, *Cancer magister*, under laboratory conditions. Journal of Crustacean Biology,
517 21(4): 897–904.
518 Tallack, S.M.L. 2007. Escape ring selectivity, bycatch, and discard survivability in the New
519 England fishery for deep-water red crab, *Chaceon quinquedens*. *ICES Journal of Marine*
520 *Science*, **64**: 1579–1586.
521 Wahle, R.A., Bergeron, C.E., Chute, A.S., Jacobson, L. D. & Chen, Y. 2008. The Northwest
522 Atlantic deep-sea red crab (*Chaceon quinquedens*) population before and after the onset
523 of harvesting. *ICES Journal of Marine Science*, **65**: 862–872.

524 Wigley, R.L., Theroux, R.B. & Murray, H.E. 1975. Deep sea red crab, *Geryon quinquedens*,
525 survey off northeastern United States. *Marine Fisheries Review* **37**: 1–21.

List of captions

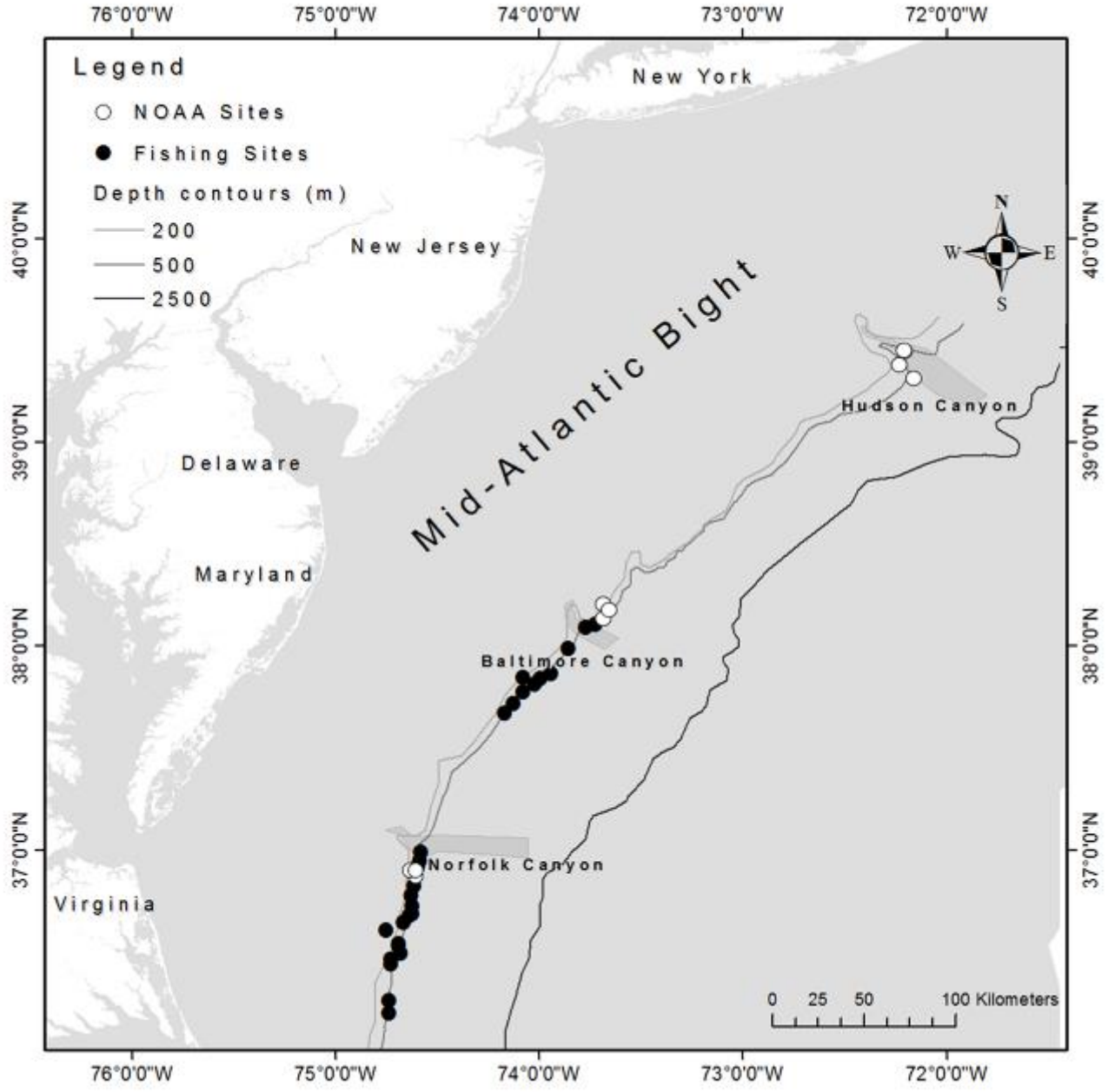

Figure 1. Location of sampling sites for red deep-sea crab, *Chaceon quinquedens*, during cruises aboard NOAA research vessels (2011–2013) and The Atlantic Red Crab Co. F/V *Hannah Boden* (2014–2016) in the Mid-Atlantic Bight.

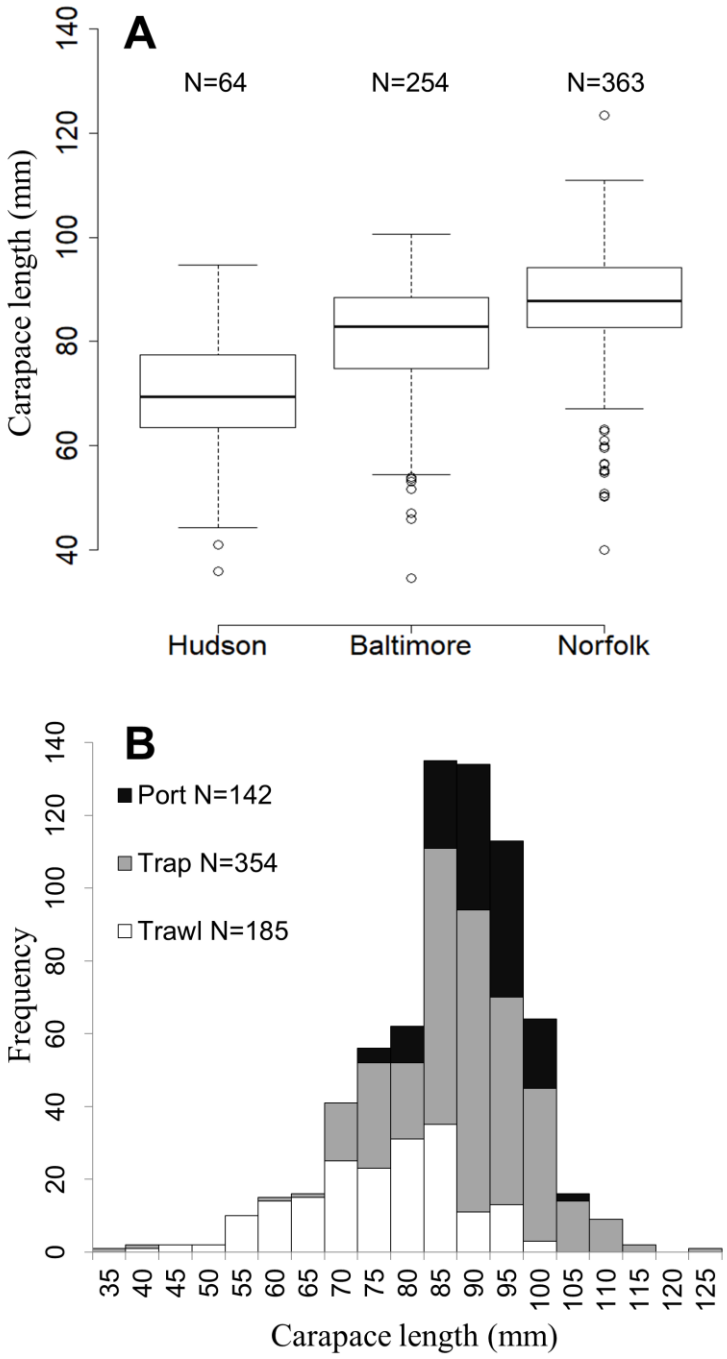

Figure 2. Mean size of female *Chaceon quinquedens* at each site sampled during 2011–2016 in the Mid-Atlantic Bight (N = 681) (**A**). Size frequency of the females collected by each sampling method (**B**).

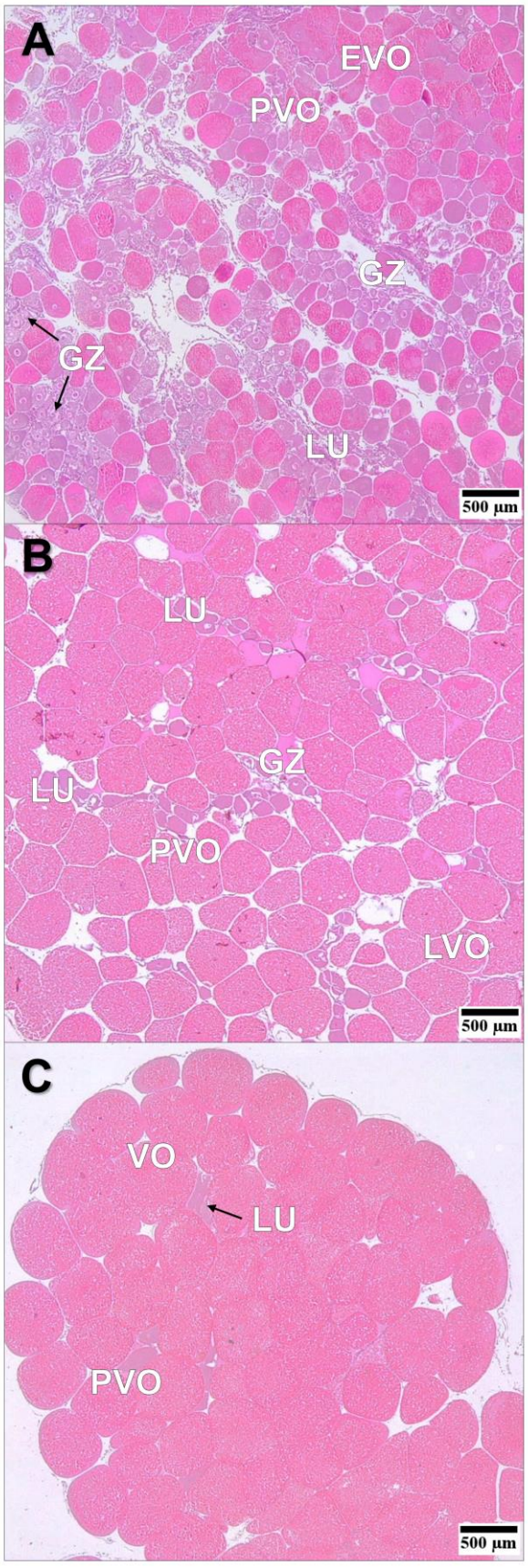

11

Figure 3. Comparisons of stages of ovarian development of *Chaceon quinquedens* females sampled during 2011–2016 in the Mid-Atlantic Bight. Ovary at the early maturing stage with a noticeable germinal zone with primary and secondary oocytes in the center and surrounded by previtellogenic and early vitellogenic oocytes (**A**). Late maturing stage with linear extensions of lumen and reduced germinal zones compared to the previous stage (**B**). Ovary at mature stage mostly filled with vitellogenic oocytes (**C**). GZ, germinal zone; LU, lumen; PVO, previtellogenic oocyte; EVO, early vitellogenic oocyte; LVO, vitellogenic oocyte; VO, vitellogenic oocyte. Scale bars: 500 µm.

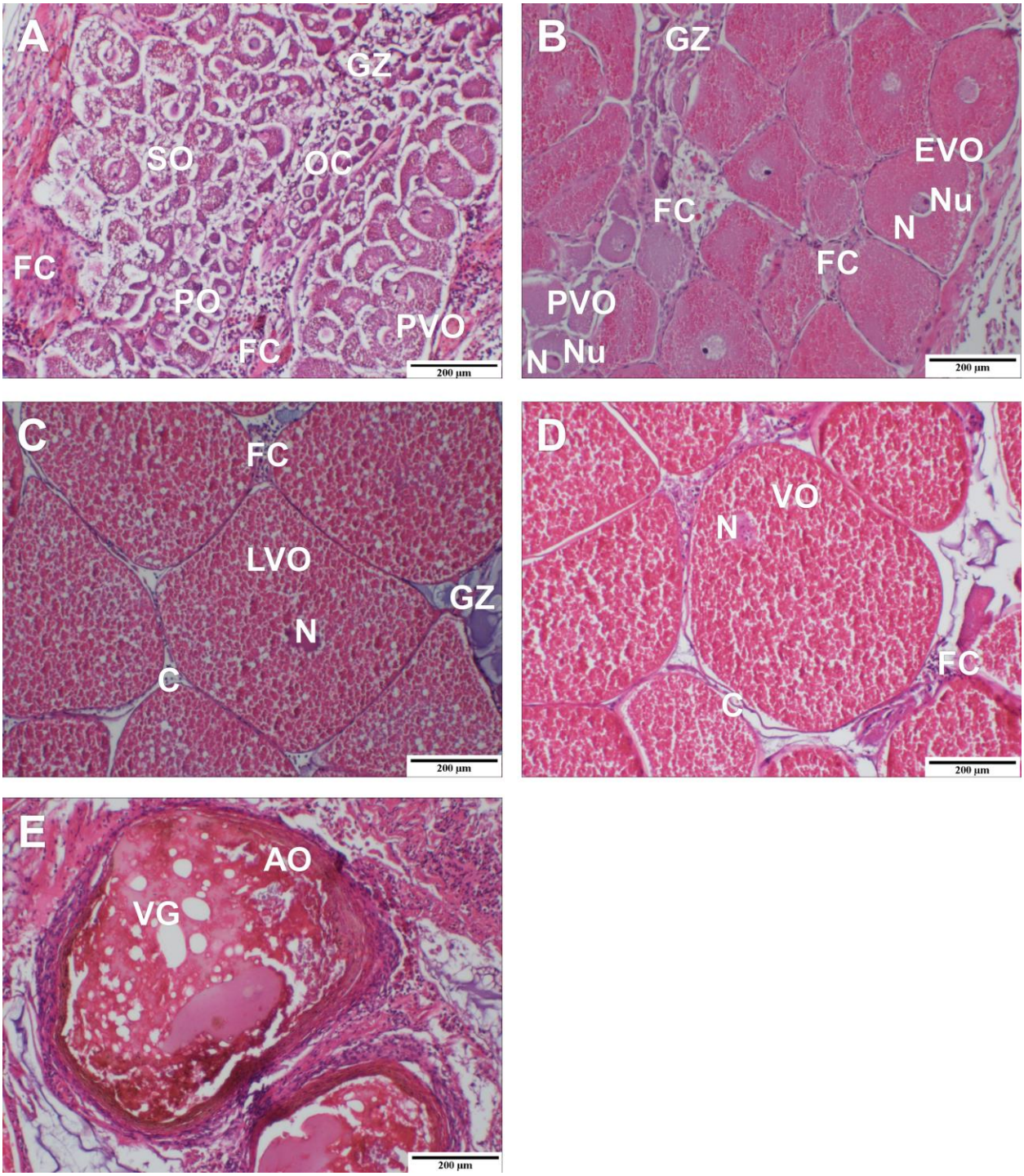

Figure 4. Stages of ovarian development of *Chaceon quinquedens* females sampled during 2011–2016 in the Mid-Atlantic Bight. Immature stage (**A**). Early maturing stage (**B**). Late maturing stage (**C**). Mature stage (**D**). Redeveloping stage (**E**). OC, oogonial cells; PO, primary oocyte; SO, secondary oocyte; PVO, previtellogenic oocyte; VG, vacuolated globules; N,

nucleus; Nu, nucleolus; FC, follicle cells; EVO, early vitellogenic oocyte; LVO, late vitellogenic oocyte; VO, vitellogenic oocyte; AO, atretic oocyte; C, chorion. Scale bars: 200 μm.

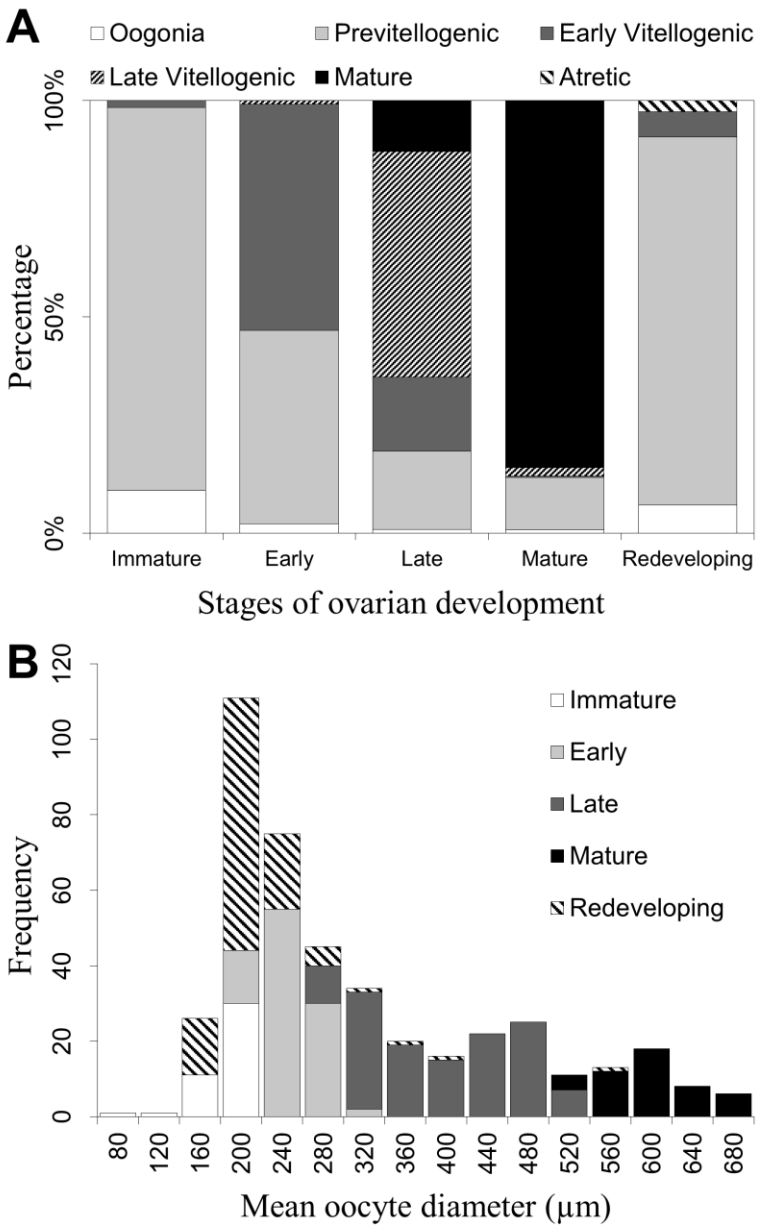

63

64 **Figure 5.** Oocyte development stages in the ovarian development stages of *Chaceon*

65 *quinquedens* in the Mid-Atlantic Bight suggesting a continuous maturation of oocytes in the

66 ovary (**A**). Frequency of mean oocyte diameter (µm) in the stages of ovarian development (**B**).

67

68

69

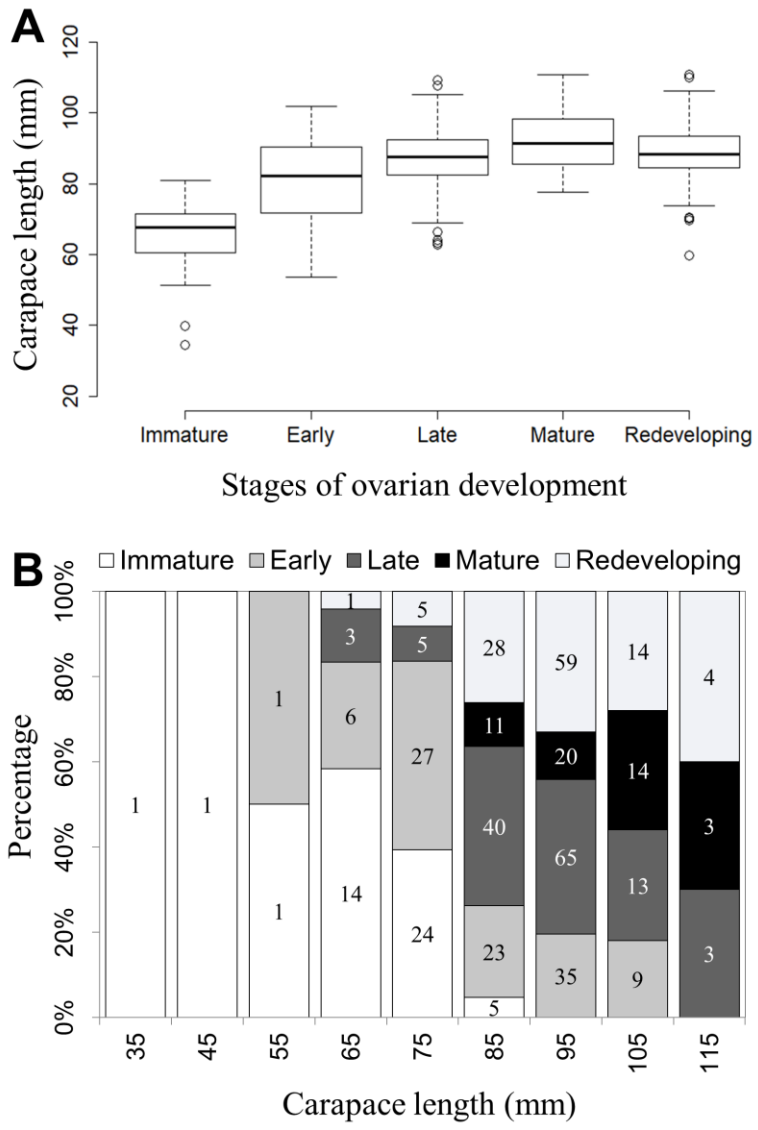

Figure 6. Carapace length (mm) of female *Chaceon quinquedens* at each stage of ovarian development sampled during 2011–2016 in the Mid-Atlantic Bight (*N*=435) (**A**). Boxes enclose central 50% of data; horizontal line is median; vertical bars delimit observations within 1.5 box lengths, whereas circles represent outliers. Percentage of ovarian development stages as a function of carapace length of females (**B**).

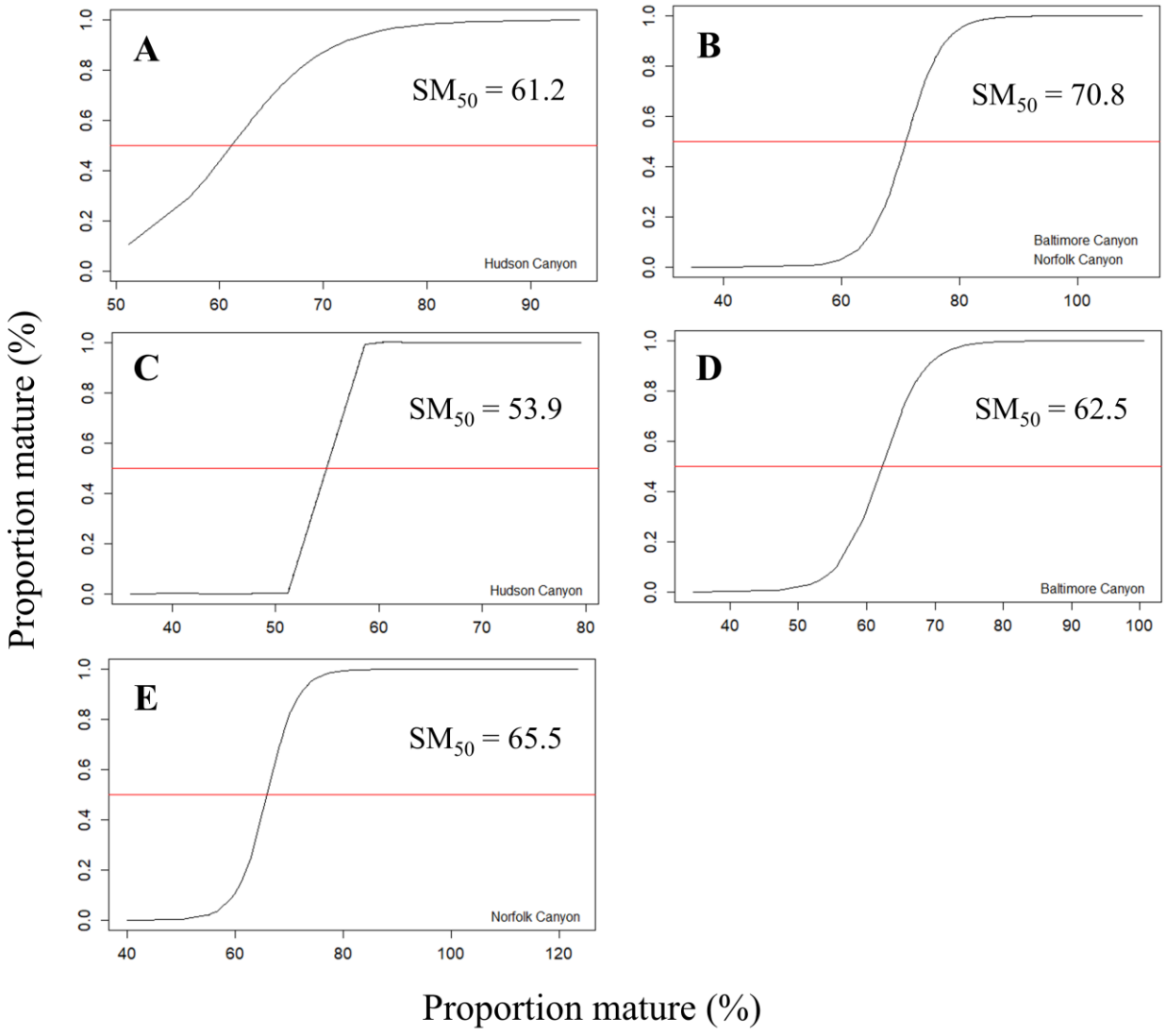

79

80 **Figure 7.** Logistic curves fitted to the physiological and behavioral sexual maturity of *Chaceon*
81 *quinquedens* females sampled during 2011–2016 in the Mid-Atlantic Bight. The horizontal line
82 represents the proportion of 50% sexually mature. Physiological maturity: Hudson Canyon (**A**)
83 and Baltimore and Norfolk canyons (**B**). Behavioral maturity: Hudson Canyon (**C**), Baltimore
84 Canyon (**D**), and Norfolk Canyon (**E**). SM_{50}, size at 50% sexual maturity.

85

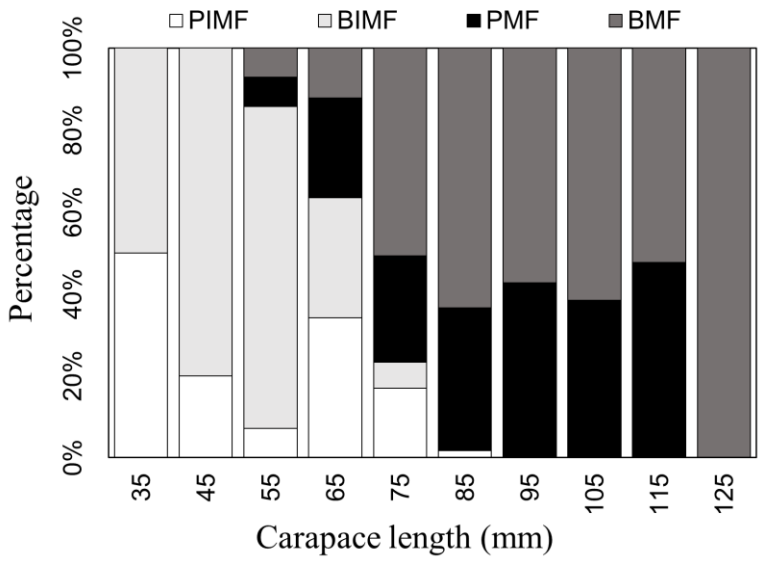

Figure 8. Size-frequency distributions of physiologically and behaviorally immature and mature females of *Chaceon quinquedens* in the Mid-Atlantic Bight. PIMF, physiologically immature females; BIMF, behaviorally immature females; PMF, physiologically mature females; BMF, behaviorally mature females.

Table 1. Data collected of *Chaceon quinquedens* aboard NOAA research vessels (R/V) and The Atlantic Red Crab Co. fishing vessel (F/V) *Hannah Boden* in the Mid-Atlantic Bight. CL, carapace length.

Year	Season	Month	Collection Method	Vessel	Geographic Location	Depth (m)	Min CL (mm)	Max CL (mm)	*N*
2011	Winter	January	Trawl	R/V	Hudson	499–632	57.1	94.7	48
2012	Winter	January	Trawl	R/V	Hudson	298	36.0	51.2	12
2012	Winter	January	Trawl	R/V	Baltimore	571	45.8	90.2	4
2012	Winter	January	Trawl	R/V	Norfolk	522–774	50.2	76.7	11
2013	Summer	July	Trawl	R/V	Hudson	792	58.7	79.5	84
2013	Summer	July	Trawl	R/V	Baltimore	289–501	65.1	97.4	12
2013	Summer	July	Trawl	R/V	Norfolk	414–750	50.3	94.5	14
2014	Summer	July	Round trap	F/V	Norfolk	> 600	70.3	110.9	69
2014	Fall	September	Round trap	F/V	Norfolk	> 600	68.3	123.4	66
2015	Summer	July	Round trap	F/V	Norfolk	> 600	39.9	108.7	61
2016	Winter	February	Round trap	F/V Port	Norfolk	> 600	83.3	98.6	12
2016	Spring	March	Round trap	F/V Port	Norfolk	> 600	85.5	97.7	4
2016	Spring	April	Round trap	F/V Port	Norfolk	> 600	70.2	97.5	19
2016	Spring	May	Round trap	F/V Port	Norfolk	> 600	73.4	86.8	10
2016	Summer	July	Round trap	F/V Port	Norfolk	> 600	75.8	99.0	42
2016	Summer	August	Round trap	F/V	Baltimore	> 600	34.6	100.5	158
2016	Fall	September	Round trap	F/V Port	Norfolk	> 600	79.2	95.0	16
2016	Fall	November	Round trap	F/V Port	Norfolk	> 600	74.4	100.9	22
2016	Winter	December	Round trap	F/V Port	Norfolk	> 600	82.3	103.0	17

Table 2. Model selection table for physiological size at maturity of female *Chaceon quinquedens* sampled during 2011–2016 in the Mid-Atlantic Bight. Model indicates the parameters used in the model, where CL50 is the carapace length at 50% maturity and *s* is the slope. N and S refer to north (Hudson Canyon) and south (Baltimore and Norfolk Canyons) sites, respectively. No, H and B refers to Norfolk Canyon, Hudson Canyon and Baltimore Canyon, respectively. K is the number of parameters for each model and AIC_C is the Akaike's Information Criterion corrected for sample size that was used to determine the best-fit model.

Model	Parameters	K	AIC_c	Δ AIC_c	Likelihood	AIC_c weight
1	CL_{50}(N), CL_{50}(S), *s*(N), *s*(S)	4	142.6	0.0	1.0	0.3
2	CL_{50}(N), CL_{50}(S), *s*	3	142.7	0.1	1.0	0.3
3	CL_{50}(No), CL_{50}(H), CL_{50}(B), *s*(No), *s*(H), *s*(B)	6	143.8	1.1	0.6	0.2
4	CL_{50}(No), CL_{50}(H), CL_{50}(B), *s*	4	144.2	1.6	0.5	0.2
5	CL_{50}, *s*	2	161.3	18.6	0.0	0.0
6	CL_{50}, *s*(N), *s*(S)	3	163.3	20.7	0.0	0.0
7	CL_{50}, *s*(No), *s*(H), *s*(B)	4	165.1	22.4	0.0	0.0

Table 3. Model selection table for behavioral size at maturity of female *Chaceon quinquedens* sampled during 2011–2016 in the Mid-Atlantic Bight. Model indicates the parameters used in the model, where CL50 is the carapace length at 50% maturity and *s* is the slope. N and S refer to north (Hudson Canyon) and south (Baltimore and Norfolk Canyons) sites, respectively. No, H and B refers to Norfolk Canyon, Hudson Canyon and Baltimore Canyon, respectively. K is the number of parameters for each model and AIC_C is the Akaike's Information Criterion corrected for sample size that was used to determine the best-fit model.

Model	Parameters	K	AIC_c	Δ AIC_c	Likelihood	AIC_c weight
1	CL_{50}(No), CL_{50}(H), CL_{50}(B), *s*	4	77.6	0.0	1.0	0.4
2	CL_{50}(N), CL_{50}(S), *s*	3	78.2	0.5	0.8	0.3
3	CL_{50}(N), CL_{50}(S), *s*(N), *s*(S)	4	79.3	1.6	0.4	0.2
4	CL_{50}(No), CL_{50}(H), CL_{50}(B), *s*(No), *s*(H), *s*(B)	6	80.6	3.0	0.2	0.1
5	CL_{50}, *s*	2	85.0	7.4	0.0	0.0
6	CL_{50}, *s*(N), *s*(S)	3	86.7	9.1	0.0	0.0
7	CL_{50}, *s*(No), *s*(H), *s*(B)	4	88.3	10.7	0.0	0.0